

Investigation of power quality issues in 14-bus electrical network with high penetration of renewable generation

Malcolm Isaac Fernandez¹ · Yun li Go¹

Received: 16 August 2023 / Accepted: 28 November 2023

Published online: 09 December 2023

© The Author(s) 2023 [OPEN](#)

Abstract

Power quality issues arise in electrical networks when variable renewable energy (VRE) is integrated into them due to their random and intermittent nature which depends on weather conditions and other factors. The variation of solar irradiance throughout the day affects the energy produced by solar panels and the integration of solar power into electrical networks will result in changes and fluctuations in the voltage profile of buses. Reactive power compensation is required to improve the bus voltage levels of the electrical network to be within the required limits and the optimal allocation of reactive power compensation devices in the network is a complex problem to be investigated for the optimum injection of reactive power to obtain better voltage profiles for the entire network. This research investigated the penetration of variable solar energy into an electrical network in terms of voltage and reactive power flow. A variety of literature was reviewed in the scope of reactive power management in power systems and a gap in addressing the optimal allocation of compensation devices in the IEEE-14 bus was addressed based on the proposed methods followed by discussions of the results in terms of voltage profiles and reactive power flow in the buses. The objective is to produce an output power of higher quality and reliability for the loads so that intermittent sources of renewable energy can be more competent with energy sources such as fossil fuels that do not depend on weather conditions. Integration of methods using compensation optimisation (optimal allocation of capacitors) and volt-var regulation (smart inverter) to improve the voltage profile that was dropped and the fluctuations after penetration of solar power were carried out. A solar bus with variable energy generation was connected to the IEEE-14 bus to study the voltage variations. This was executed by the power flow calculation module to determine the voltages and reactive power in the buses of the network. With the optimum allocation of the capacitors, the voltage levels in all weak buses of the IEEE-14 bus were increased to be between 0.95 p.u. and 1.05 p.u. which was the voltage specifications of the Malaysian Grid Code Requirements. The voltage for every weak bus in the IEEE-14 bus showed a rise of 5.7% from 7 a.m. to 12 p.m. With that, the volt-var function was used for reactive power regulation at the point of common coupling (PCC) and a reduction of voltage deviation of 2.828 to 1.3% in the IEEE-14 bus was observed. The average voltage profile of all buses managed to attain a value of 98.99% from 95.673% (with solar power) with the optimal allocation of capacitors and volt-var regulation. The beneficiaries of this project will be the Sustainable Energy Development Authority (SEDA) which administers the Net Energy Metering (NEM) scheme and Tenaga Nasional Berhad (TNB) which is the Malaysian multinational electrical company focused primarily on the generation, transmission, and distribution of electricity in Peninsular Malaysia. The Energy Commission and Ministry of Energy and Natural Resources are also beneficiaries as they carried out a competitive bidding programme for large-scale solar (LSS) known as the LSS@MEntARI or LSSPV4 to attain bids for the development of around 1000 MW AC of LSS power plants to be operational in Malaysia by 2022. This work will also be beneficial in future research in planning

✉ Yun li Go, y.go@hw.ac.uk | ¹School of Engineering and Physical Sciences, Heriot-Watt University Malaysia, 1, Jalan Venna P5/2, Precinct 5, 62200 Putrajaya, Wilayah Persekutuan Putrajaya, Malaysia.



reactive power compensation devices in networks of multiple VRE sources, communication, and coordinated control of smart inverters, and incorporation of these devices for smart grid applications.

Keywords Power Flow · Compensation · Optimal allocation · Volt-var

1 Introduction

Malaysia's equatorial location implies that it has great potential for the implementation of large-scale solar power projects as the irradiance levels of the country are relatively high throughout the year. Around 1575 to 1812 kWh/m² of solar irradiance is received in Malaysia and this has close values to Southeast Asia's average solar irradiance value which is 1500 to 2000 kWh/m² [1]. Despite the high potential for solar power penetration into the electrical grid, the integration of solar PV feeders has faced distinct challenges and many methods for improving its power penetration have been researched and developed through the years. The variation in solar irradiance and atmospheric temperature affects the generation profile of solar panels. These variables are intermittent and not consistent throughout the atmosphere in a specific location and this will cause a generation of electricity that is fluctuating as well. This variation of the two parameters mentioned is due to the dispersion and blocking of sunlight by clouds in what is known to be the shading effect and this is the major reason why solar generation is intermittent [2]. An element of volatility and randomness also exists in solar PV technology in which its generating efficiency will decline over the years due to aging and coverage of dust. Bird passing and climate change frequency also cause a rapid change in generated power [3].

With this, voltage stability will arise in the electrical network buses integrated with solar panels. In the research conducted in [4], it was found that the location of solar panels had a major role in the improvement of the stability of the power system. Next, it was also discussed that installed solar panels on a weak bus operated at a lagging or leading power factor of 0.7 in a stable system. Lastly, fluctuations in the frequency of the power system can also happen due to mismatching in load and generation. In intermittent sources of renewable energy, there is an important characteristic known as the lack of providing inertia or rotor angle when it is required. Generators of solar PV do not work like synchronous generators in which the rotating mass is operated directly proportional to the frequency of generation which controls the load change [5]. An ideal generation station must be equipped with inertia in which there is a change in frequency, then mitigation of this problem by devices such as batteries, capacitors, and ultracapacitors, can be executed and more of this research was carried out in [6]. The research highlight will be focused on the management of reactive power using capacitor banks and smart inverters in solar panels. Voltage regulation in buses, power loss reduction, power factor correction, and power quality improvement are the positive impacts of connecting capacitors in distribution systems. The optimal allocation of capacitors is a complex problem as it has a combinatorial nature and the size of capacitors as well as the location of their placement are discrete variables that will result in different outcomes of power flow in electrical networks. The optimal allocation of capacitors will be formulated by the desired voltage limits of 0.95 p.u. to 1.05 p.u so that the module will find the best possible configuration of capacitors in terms of its rating and location to obtain the specified range of voltage in all buses of the IEEE-14 bus.

2 Review of literature on reactive power flow in electrical networks

A power system study focusing on voltage profile variations after the integration of solar power into the IEEE-9 bus was carried out by [7]. The problem statement here is that PV systems will result in an impact on the voltage stability of power systems due to the intermittent nature of solar irradiance. This research aim was done using PVsyst to determine and optimal sizing of the PV modules based on real data of the installation of LSS in various locations. After this, power system analysis was carried out by using the PSS SINCAL software which is a simulation tool for power systems to run a load flow analysis to analyse the variation in potential difference on each bus when connected to the IEEE-9 bus power system. From the load flow analysis, the researchers found that among the 9 buses, the stable configuration for integrating the solar PV will be at bus 4 due to the small voltage deviations at the affected buses.

Researchers in [8] carried out a power system analysis to compare the performance of reactive power compensation devices which were STATCOM and the static VAR compensator (SVC) on static voltage stability of large-scale PV integration in the IEEE-14 bus system. This research aim was achieved by using the Q-V modal analysis method by implementing it in MATLAB and Power System Analysis Toolbox (PSAT). The key findings in this study were that in

comparison with the SVC, the STATCOM provided a much better option to improve the stability of the voltage in large-scale PV systems. This was because the STATCOM resulted in higher system loading margins in all the cases. Furthermore, placing SVCs in PV generator buses is much more effective in improving the voltage stability of the system compared to placing it at the weakest bus as well as placement which deals with short-term dynamic reactive power support.

Research carried out in [9] investigated the effects of LSS on the quantitative and qualitative voltage characteristics by short-term and long-term state variables using the IEEE-14 bus transmission network. This aim was achieved by using a formulated mechanism to analyse the dynamic phenomenon of voltage instability with the integration of LSS. These simulations were done using the PSAT using eigenvalues from the reduced non-singular Jacobian matrix. In addition, it was also found that the static analysis overestimated the margin of stability which means that dynamic analysis is important to define the critical time of control application for appropriate corrective actions. PV units influence the stability of dynamic voltage and this depends on the settings and type of controllers incorporated in the systems of the PV module.

Research in [10] designed and implemented an optimised version of a static VAR compensator (SVC) and tap changer (TC) to reduce reactive power as well as the number of operations in the tap changer. The altering of the parameters such as gain, settling time, dead band time delay, and triggering compensator pulse of the on-load tap changer (OLTC) resulted in an optimum number of TC operations which demonstrated an improvement in voltage profile. The SVC model for the improvement of the voltage profile was carried out in MATLAB. Without the SVC model, the simulation results showed that the regulated voltage was within the range of 0.967 ± 0.005 p.u. when the number of tap changer operations was 9 times. When the SVC model was integrated for absorption and injection of reactive power, the results simulated in Simpower demonstrated that the voltage profile was improved to around 0.98 ± 0.005 p.u. and the number of TC operations was reduced to 5. From this research, the level of voltage variations was reduced as well as the number of TC operations by implementing the SVC in the system.

Authors in [11] researched the theory of instantaneous reactive power by the implementation of the hysteresis current controller. The control system that was proposed contained the instantaneous reactive power theory (IRPT) which is based on the current source inverter (CSI) to reduce the reactive power as well as the harmonic currents. This simulation was carried out in MATLAB/SIMULINK to use the control scheme of grid-connected PV systems to improve the power factor to a nearly perfect level close to unity. The aim was achieved by implementing an IRP-based control algorithm with a grid-tied inverter having active power as well as reactive power control. When a basic R-L load was connected to the grid, its power factor was 0.9285 and this was reduced to 0.7808 when a solar PV with unity power factor was integrated with it with 50% of load sharing. In the third case, the power factor was then improved to 0.9864 when the IRPT and hysteresis controller were incorporated.

Based on research in [12], results were simulated by using the "RastrWin 3" software package to study the influence of various FACTS devices and OLTC installed in transmission grids by the reconfiguration of reactive power flow and the net power loss based on the model known as the United Energy System (UES) of Russia in the 110 kV to 500 kV networks for two distinct conditions which are winter maximum and summer minimum for 2016. The key findings were that the range of variation in active power losses was highly dependent on the position of the OLTC. This range of active power losses was higher in the 500 kV substations as compared to the 220 kV substations for both conditions of winter maximum and summer minimum based on the results. As in the use of FACTS devices and capacitor banks, this research paper found that the injection of reactive power in the energy scheme to reduce the total losses in UES was not practical because the lines were not loaded to natural power to generate reactive power, which creates an exceeded amount in the grid which will then lead to overcompensation and an added increase in the loss of active power due to additional generation. From the results, the total reduction in losses in the UES was the highest for OLTC, followed by capacitor banks and then the controlled shunt reactor.

Research carried out in [13] investigated voltage profiles of the IEEE-9 bus with the integration of LSS power and improvement of these profiles by using FACTS devices for reactive power compensation by using PSS/E. Research in [14] studied the support of reactive power in prosumer grids with solar power and found that the Python-based optimal capacitor placement algorithm did not create overvoltage and power loss issues. The optimal allocation of capacitors and distributed generators by using probabilistic generation models in MATLAB was investigated in [15]. PV inverters and fixed capacitors for the management of reactive power were researched in [16] and found that they reduced the losses of energy in a real low-voltage distribution grid. Research in [17] investigated the optimal allocation of FACTS devices for the IEEE-30 bus system integrated with stochastic renewable energy power using new metaheuristic optimisation methods.

2.1 Contribution

To complement the research carried out in [7] and [9], further analysis was carried out to study the fluctuation and drops of voltage profile on a time series basis throughout 24 h in a day. This involved the injection of a time-varying load profile of solar power into the IEEE-14 bus on a case-by-case basis to find out the worst-case scenario of interconnection in terms of voltage drop. The volt-var regulation and the compensation optimisation iteration algorithm for optimal capacitor allocation were used to improve the voltage profile of all buses in the IEEE-14 bus system. Based on research carried out by [18], the volt-var control modelling of the solar bus was adapted and tested with altering parameters of the QU (reactive power-voltage) and PQ (active power-reactive power) functions to get optimum results of voltage and this incorporated to function together with the optimal capacitor placement to improve the voltage fluctuation and levels.

Furthermore, the contribution of this research was based on research in [19] in which compensation methods were used to improve voltage profiles in the IEEE-9 bus. The results in [19] were the optimal capacitor placement method, the voltage profile for all buses was improved to be within 0.94 p.u. to 1.01 p.u. The average voltage profile for all buses of the IEEE-9 bus demonstrated an increase of 13.3% as taken from 7 a.m. to 12 p.m. The volt-var regulation was implemented in the solar bus for the regulation of reactive power at the point of common coupling (PCC), this resulted in a voltage fluctuation reduction of 2.71 to 0.81% in the IEEE-9 bus. The results in [19] were used as verification of results obtained in terms of the percentage of improvement in voltage profile levels and the percentage of reduction in voltage fluctuations throughout the day. In this research, a separate case study and in-depth analysis of the IEEE-14 bus test system will be carried out to compare the consistency and pattern of the results of reactive power flow and the changes in the voltage profile of the buses. The method of optimal allocation of capacitors in the IEEE-14 bus and a smart inverter with a volt-var function in the solar bus is used. The improvement of the voltage levels, voltage deviation, and reactive power reduction will be analysed for the IEEE-14 bus.

3 Methodology

The time-varying load profile of the solar bus was integrated with the IEEE-14 bus in PSS SINCAL. The optimal allocation of the capacitor's module was used to calculate the reactive power demand in the buses and it determines the optimal location and rating of capacitors with reference to the voltage limits which were initially set to be within the Malaysian Grid Code Requirements [20]. The power flow and compensation optimisation module for the optimal allocation of capacitors was developed by Siemens [21, 22] in PSS SINCAL software and these modules were used in this research. The volt-var function was then modelled in the solar bus controller settings for further improvement in voltage fluctuations over an annually average 24-h period and this will be executed together with the bus topology that has already had its reactive power compensated by the capacitor banks to compare the voltages during peak hours of solar power penetration. This research was done to optimise the models of the buses for photovoltaic system-based DC-in feeders to model the solar farm of 116 MWp. The interfaced buses with the solar bus were buses 4, 5, 7, 9, 10, 11, 12, 13, and 14 to determine the worse scenarios for compensation optimisation procedures.

3.1 The IEEE-14 bus

The IEEE-14 bus is a representation of a simple approximation in the American power system and it consists of 5 generators, 14 busses, and 11 loads as presented in Fig. 1. Data on loads, generators, buses, transformers, and lines were obtained from the standardized IEEE-14 bus data sheet. The base apparent power of this test system is 100 MVA and the data on tables are referenced based on this value. Based on the IEEE-14 Bus Datasheet [23], the voltage levels for this topology are 69 kV (bus 1 to bus 5), 18 kV (bus 7 and bus 8), and 13.8 kV (bus 9 to bus 14). Table 1 shows all the line data of resistance and reactance with its MVA rating and Table 2 shows the load parameters. Figure 2 shows the IEEE-14 bus after power flow calculation was executed.

Data such as generator MVA and transformer tap setting value (p.u.) were all included to be modelled manually in addition to this line and load data tables as shown above. Specific data were obtained and modelled accordingly in PSS SINCAL in accordance to the datasheet [23].

Fig. 1 Sequence of optimal capacitor allocation for IEEE-14 bus based on [22]

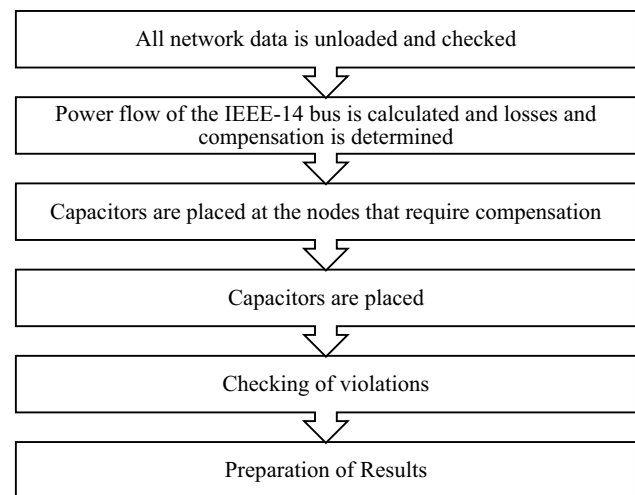


Table 1 IEEE-14 bus line parameters [23]

Line number	From bus	To bus	Line resistance (pu)	Line reactance (pu)	Half-line charging susceptance (pu)	MVA rating
1	1	2	0.01938	0.05917	0.02640	120
2	1	5	0.05403	0.22304	0.02190	65
3	2	3	0.04699	0.19797	0.01870	36
4	2	4	0.05811	0.17632	0.02460	65
5	2	5	0.05695	0.17388	0.01700	50
6	3	4	0.06701	0.17103	0.00640	65
7	4	5	0.01335	0.04211	0	45
8	4	7	0	0.20912	0	55
9	4	9	0	0.55618	0	32
10	5	6	0	0.25202	0	45
11	6	11	0.09498	0.1989	0	18
12	6	12	0.12291	0.25581	0	32
13	6	13	0.06615	0.13027	0	32
14	7	8	0	0.17615	0	32
15	7	9	0	0.11001	0	32
16	9	10	0.03181	0.0845	0	32
17	9	14	0.12711	0.27038	0	32
18	10	11	0.08205	0.19207	0	12
19	12	13	0.22092	0.19988	0	12
20	13	14	0.17093	0.34802	0	12

3.2 Power flow calculation

Power flow or load flow is used to calculate the operating behaviour of transmission and distribution networks. This can be divided into symmetrical or unbalanced power flow but the symmetrical power flow will be used as the individual real power of the 3-phase loads that are set to be equally shared across the phases. There are methods of iteration known as the Newton–Raphson method or the current iteration which are the only remaining methods. Generators and loads which are active network elements are reproduced with their voltage and current sources. Voltages and currents in the scheme are assumed to be from sources of voltages and currents. Therefore, the process of iteration is a procedure done to alter the voltages and currents where they feed into the network if it is required for the needed value of accuracy. These calculations generate a non-linear set of equations that does not contain a

Table 2 IEEE-14 bus load parameters [23]

Bus number	Load real power (MW)	Load reactive power (MVAR)
1	0	0
2	21.7	12.7
3	94.2	19.1
4	47.8	-3.9
5	7.6	1.6
6	11.2	7.5
7	0	0
8	0	0
9	29.5	16.7
10	9.0	5.8
11	3.5	1.8
12	6.1	1.6
13	13.8	5.8
14	14.9	5.0

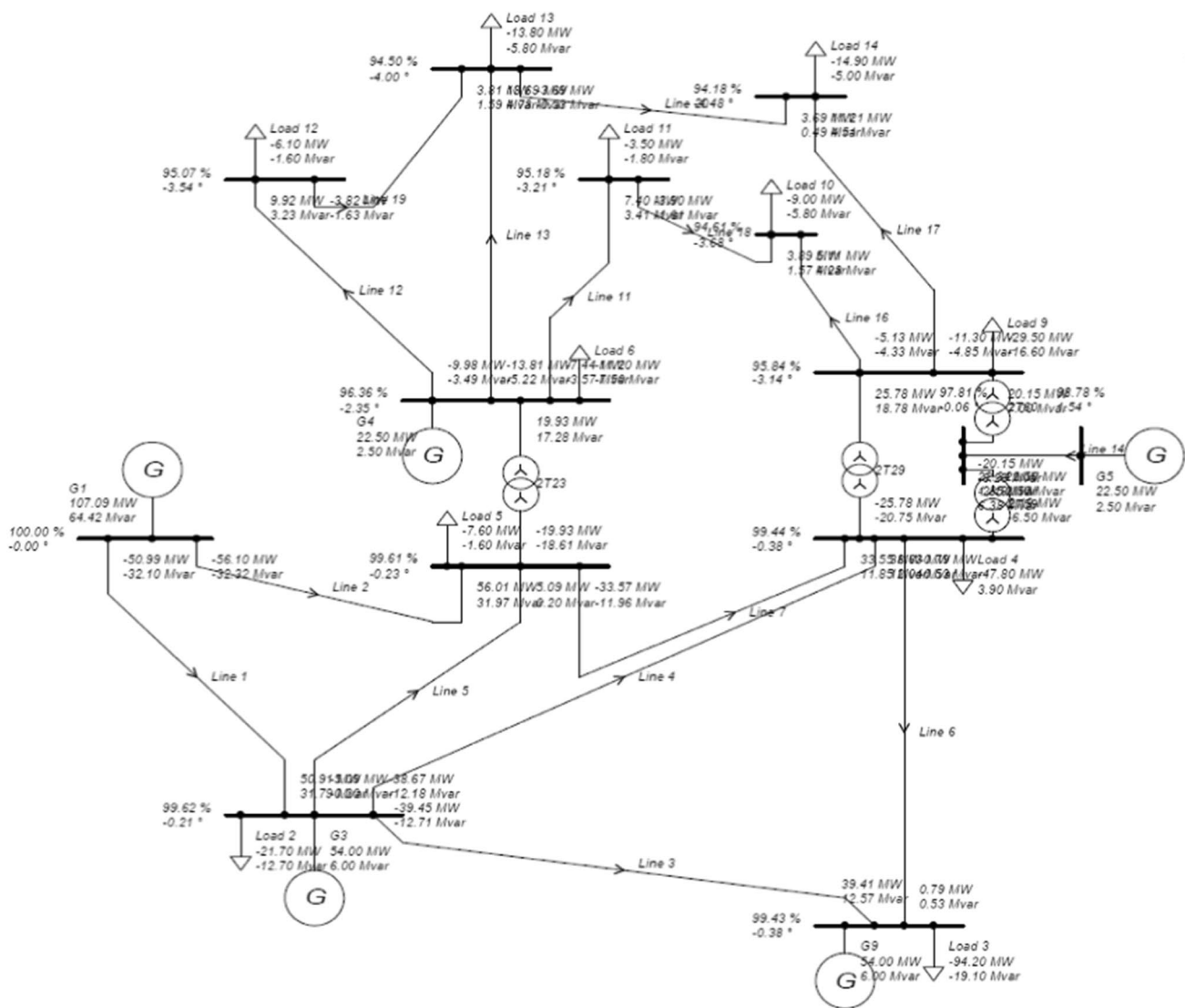


Fig. 2 The IEEE-14 Bus Topology modelled in PSS SINICAL with power flow

direct solution and the Gaussian equation is applied to solve it [21]. As a result, power flow analysis calculates the voltages and current flow resulting from power consumption at the nodes which allows users to design variations in the network to make sure the planning of the supply network is optimal. The data of voltage, current, and power for branches, nodes, generator, and load can be obtained by the power flow simulation results so that evaluation of network losses and voltage deviations can be done. These calculations can be done for any number of meshed networks and all these data are checked for topological and logical plausibility. In theory, networks with N number of nodes can have N number of equations in the connection of the complex node voltages to the complex feed power as shown in the equation below:

$$\begin{aligned} \underline{S}_i &= P_i + jQ_i = \underline{V}_i \times \sum_{k=1}^N \left(\underline{Y}_{i_k}^* \times \underline{V}_{i_k}^* \right) \\ i &= 1 \dots N \end{aligned} \quad (1)$$

The four values in each node are the node voltage angle, active feed, reactive feed, and magnitude of node voltage. This will be used to calculate power flow of the 14-bus without solar, with solar, and after the compensation procedures have been executed.

3.3 Optimal allocation of capacitors

The objective of this optimisation procedure is to reduce losses in the network by inserting capacitors. An important condition in this module is that the voltage limits and utilisation defined in the settings of calculation cannot be exceeded when the placement of capacitors is done. These voltage values were set in accordance with the Malaysian Grid Code Requirements of 0.95 p.u. to 1.05 p.u. in the option of voltage lower limit and voltage upper limit under power flow calculation settings. Optimal capacitor placement is determined by PSS SINCAL [22] by power flow series that interface different capacitors to permitted nodes. The capacitor with the highest rating available will be chosen from a pool of capacitors to be placed at the first available node. Then, the calculation of power flow and power loss analysis in the network will be executed. By using active losses of individual branches, the network losses P_l are calculated using the following equation:

$$P_l = \sum_{i=1}^L P_i \Rightarrow \text{minimum} \quad (2)$$

PSS SINCAL documents the data if the losses are lesser as compared to that of the original network condition. There is an additional condition whereby the limits in the calculation settings are required to be met. If these requirements are not met, the capacitor attachment is not documented. Next, the capacitor connected to the first node is removed and connected to the next available node. Then, power flow is calculated with the determination of losses in the network. If these losses are less than the losses in the original condition of the network and all constraints have been met, then PSS SINCAL documents attach the capacitor. The loss reduction which is the difference in loss in comparison to the original network is calculated using the following equation:

$$dP_l = P_l - P_{l_{opt}} \quad (3)$$

$$dQ_l = Q_l - Q_{l_{opt}} \quad (4)$$

$$dS_l = S_l - S_{l_{opt}} \quad (5)$$

This procedure is repeated until all the available nodes for placing capacitors have been processed and then the location that produces the highest loss reduction will be determined for capacitor placement [22]. This algorithm delivers the optimal results of electrical networks in terms of bus voltage levels using automatically rated capacitors based on the optimised reactive power demand of the weakest buses. After the allocation of capacitors, the power flow analysis can be executed again to obtain a better voltage profile that is observed in all the buses as the reactive power demand has been matched in the optimum configuration.

Fig. 3 QU Function

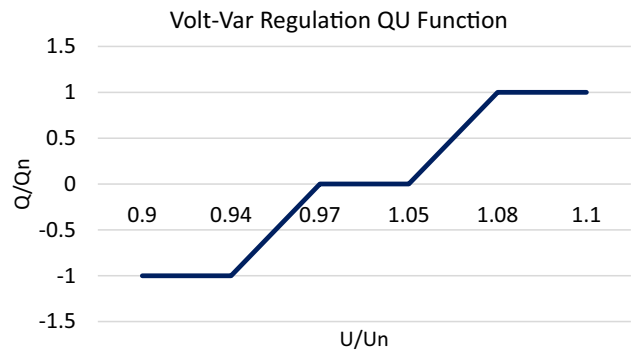


Table 3 PQ Function Parameters

Parameters	Value (p.u.)
Start voltage inductive (v1i)	1.05
End voltage inductive (v2i)	1.08
Active power (Pi/Sn)	1
Reactive power inductive (Qi/Sn)	0.4843

This procedure of capacitor placement consists of the following advantages for the network that is integrated with solar power:

- Reduces the apparent power transferred within the network.
- Places capacitors in the most optimised configuration for reactive power compensation.
- Reduces losses in the transmission network.
- Reduces the utilisation of equipment.
- Improves the voltage profile in the network.
- Aids in avoiding violations to the voltage limits as per the Grid Code Standards.

3.4 Volt-var regulation

The QU function works to keep the voltage within acceptable ranges. This function manages the output of reactive power from devices to uphold a specified voltage level. However, the PQ function regulates reactive power and real power so that the overall power flow in the grid fulfills the operational criteria. The PQ function aids in the overall equilibrium and quality of power in the electrical network. The volt-var function in the controller settings of the solar bus was modeled by the QU function in Fig. 3 for the maintenance voltage profiles in the IEEE-14 bus. This is carried out by controlling reactive power flow according to the voltage of the point of common coupling (PCC). When the voltage at the PCC drops below 0.94 p.u., there will be an active injection of reactive power by the smart inverter to increase the voltage. If the voltage drops within the range of 0.94 p.u. to 0.97 p.u., the smart inverter will inject reactive power in proportion to the rate of change so that the voltage is maintained within the normal range [18].

No contribution of reactive power occurs in the distribution system when the voltage range is between 0.97 p.u. and 1.05 p.u. However, when the voltage at the PCC increases to be between 1.05 p.u. and 1.08 p.u., there will be absorption of reactive power by the smart inverter to prevent excessive increase in voltage levels. Lastly, when the voltage increases above 1.08 p.u., the smart inverter will aid in restraining this elevation by absorption of reactive power [18]. The settings of the PQ function are specified in Table 3.

Table 4 Voltage profile of the IEEE-14 bus system without solar and its ideal case

Bus	IEEE-14 Bus without Solar (Reference Case) V/Vn [%]	Ideal Case V/Vn [%]
1	100	100
2	99.624	99.899
3	99.434	99.819
4	99.44	99.825
5	99.611	99.886
6	96.355	99.791
7	97.807	99.903
8	98.784	100.861
9	95.841	99.642
10	94.615	99.301
11	95.183	99.446
12	95.072	99.257
13	94.503	99.071
14	94.184	98.945

4 Results and discussions

4.1 Voltage profile analysis of the IEEE-14 bus

The power flow calculation was carried out for different cases of interconnection between the solar bus and the IEEE-14 bus. The reference case was selected to be the IEEE-14 bus without the connection of solar bus together with an ideal case of the IEEE 14-bus test system (without solar) with optimal allocation of capacitors as presented in Table 4. The power flow results for this reference case in terms of voltage profile (V/Vn), real power (P), reactive power (Q), and apparent power (S) in each bus was calculated.

From these results, the voltage profile of the IEEE 14-bus without solar demonstrated an approximate range that was acceptable throughout a day according to the Malaysian Grid Code Requirements as the lowest of the values was from bus 14 with 94.184%. The voltage profile in other buses ranged from 94 to 100%. Based on the reference case, the solar bus was interfaced to all the buses without synchronous generators on a case-by-case basis. This was carried out to investigate the worst-case scenario of voltage profile drop based on the peak time of day in which the voltage profile was at the minimum value. After testing each of the buses with the solar bus, the results were tabulated and the minimum value of voltage for all buses was computed to find out the worst buses of solar power interconnection. It was observed that the time of day for worst case of voltage profile violation (lowest voltage levels) in every bus was at 12 p.m. for every case of interconnection. Table 5 shows the results of average voltage profile of every bus of the IEEE-14 bus at 12 p.m. for the cases of solar bus interconnection.

Table 5 Voltage analysis of the IEEE-14 bus system when integrated with solar bus

Connection of solar bus	Average voltage (%) of all 14 buses at 12 p.m	Average voltage (p.u.) of all 14 buses at 12 p.m	Malaysian grid code requirements
Bus 4	97.1695	0.972	0.95 p.u. to 1.05 p.u
Bus 5	97.1710	0.972	
Bus 7	96.0601	0.961	
Bus 9	96.3332	0.963	
Bus 10	95.8248	0.958	
Bus 11	95.7051	0.957	
Bus 12	95.6730	0.957	
Bus 13	95.9207	0.959	
Bus 14	95.9664	0.960	

From these results, the worst-case scenario of solar bus interconnection was selected for further analysis with compensation methods and this was the interconnection case to bus 12 which resulted in the IEEE-14 bus to have an average voltage profile of 95.673% for all buses at the period of the lowest voltage. The best-case scenario however for the interconnection of solar to the 14-bus was bus 5 with an average voltage profile of 97.171% for all buses. The interconnection of solar to bus 12 resulted in minimum voltage values of 91.045%, 91.181%, and 91.661% in buses 12, 13, and 14 respectively. This violated the grid code requirements of 0.95 p.u. to 1.05 p.u. Analysis on values based on a point in time (12 p.m.) was presented in tables as the benchmark of results. However, time-series graphs of the voltage profile throughout every hour of the day in a 24-h period was illustrated for demonstration of the voltage profile improvement throughout the day.

4.2 Improvement of voltage profile by optimum allocation of capacitors

The bus voltages of the IEEE-14 bus system without solar penetration demonstrated constant levels in a straight line throughout the day as illustrated in Fig. 4. The modelled solar bus that was connected to the IEEE-14 bus had the following time-varying profile of energy injected into the grid (annual hourly averages for a period of one day) as shown in Fig. 5. After the case study of the IEEE-14 bus and solar bus, bus 12 was found to be the worst case of solar power connection as the average voltage profile across all the buses was relatively the lowest. Fluctuation and drop of voltage profile in every bus was observed except for bus 1 which remained at 1 p.u. throughout the scenarios. Bus 12, 13, and 14 showed the most drop in voltage profile reaching a minimum value of 91.045%, 91.181%, and 91.661% respectively and this can be observed in Fig. 6. After the compensation was done, voltage profile improvement was carried out as illustrated in Fig. 7. Table 6 shows the results of the optimised reactive power demand in the IEEE-14 bus in which the capacitors was placed in accordance with their rated capacity. These values are the optimised reactive power demand and capacitor ratings of these values of reactive power were placed at the respective buses specified in Table 6 to inject these values of reactive power for the overall improvement of voltage profile in the buses of the topology.

The bus with the lowest voltage profile of 91.045% which was bus 12 itself was improved to 96.161%. Bus 2, 3, and 5 were the most stable buses as there were minimal drops in voltages after solar power penetration. Table 7 summarises the comparative results of the voltage profile when the IEEE-14 in the three scenarios at 12 p.m. Figure 8 illustrates the

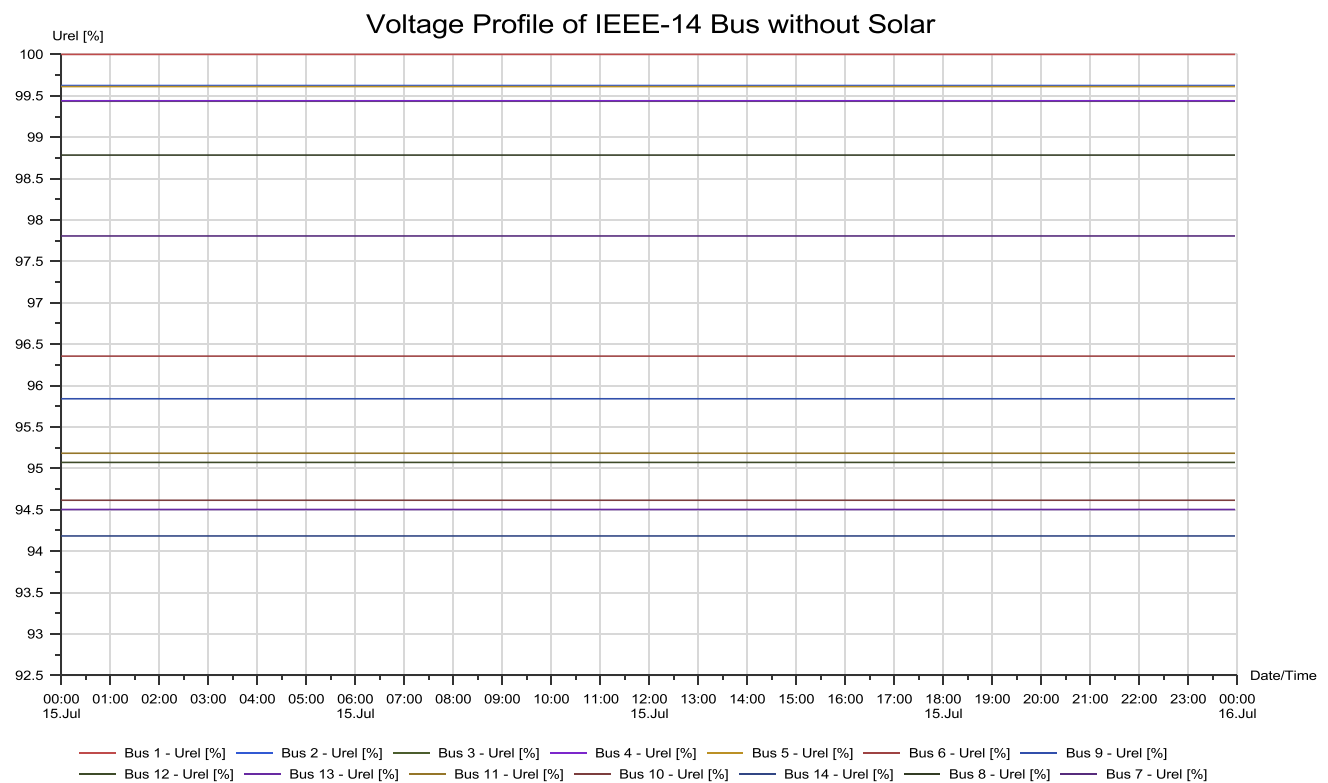


Fig. 4 Voltage profile of IEEE-14 bus without solar

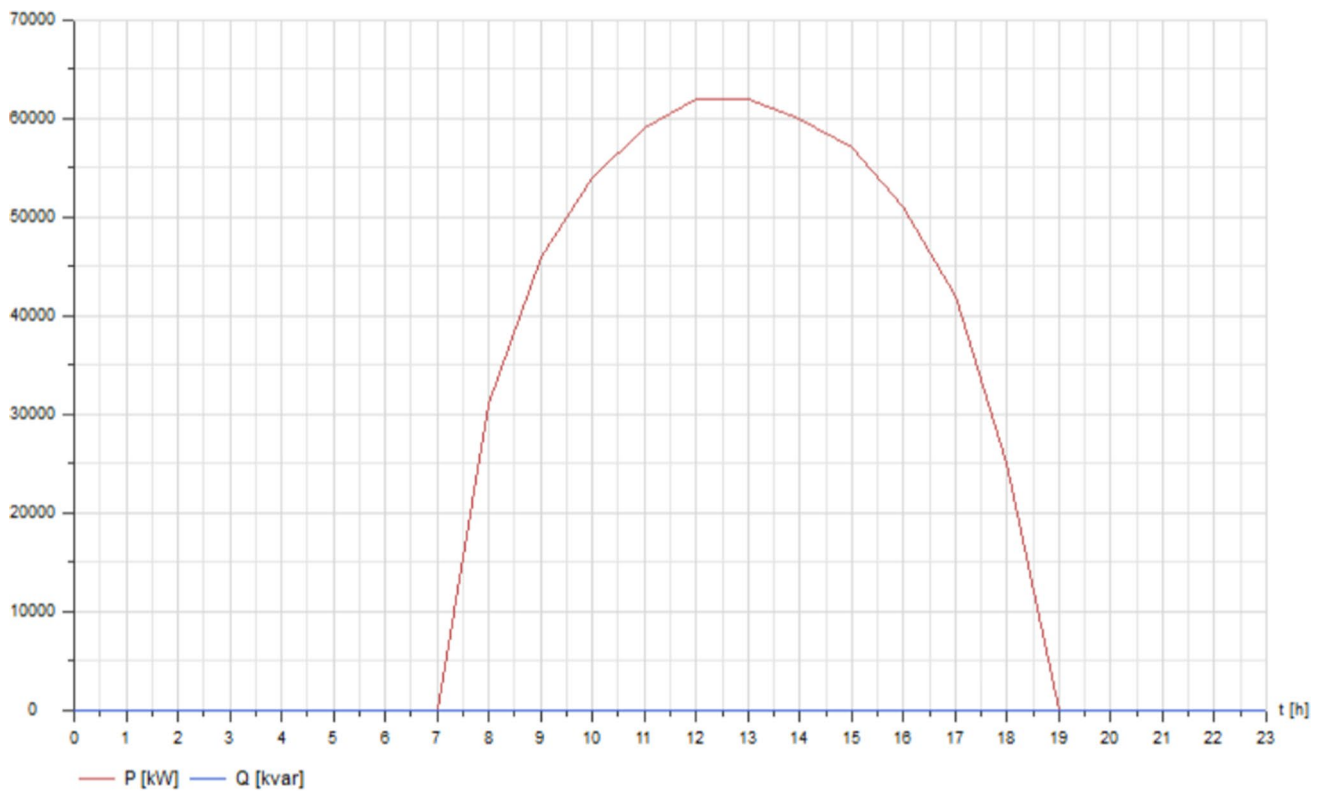


Fig. 5 Time-varying profile of energy injected by solar bus to IEEE-14 bus

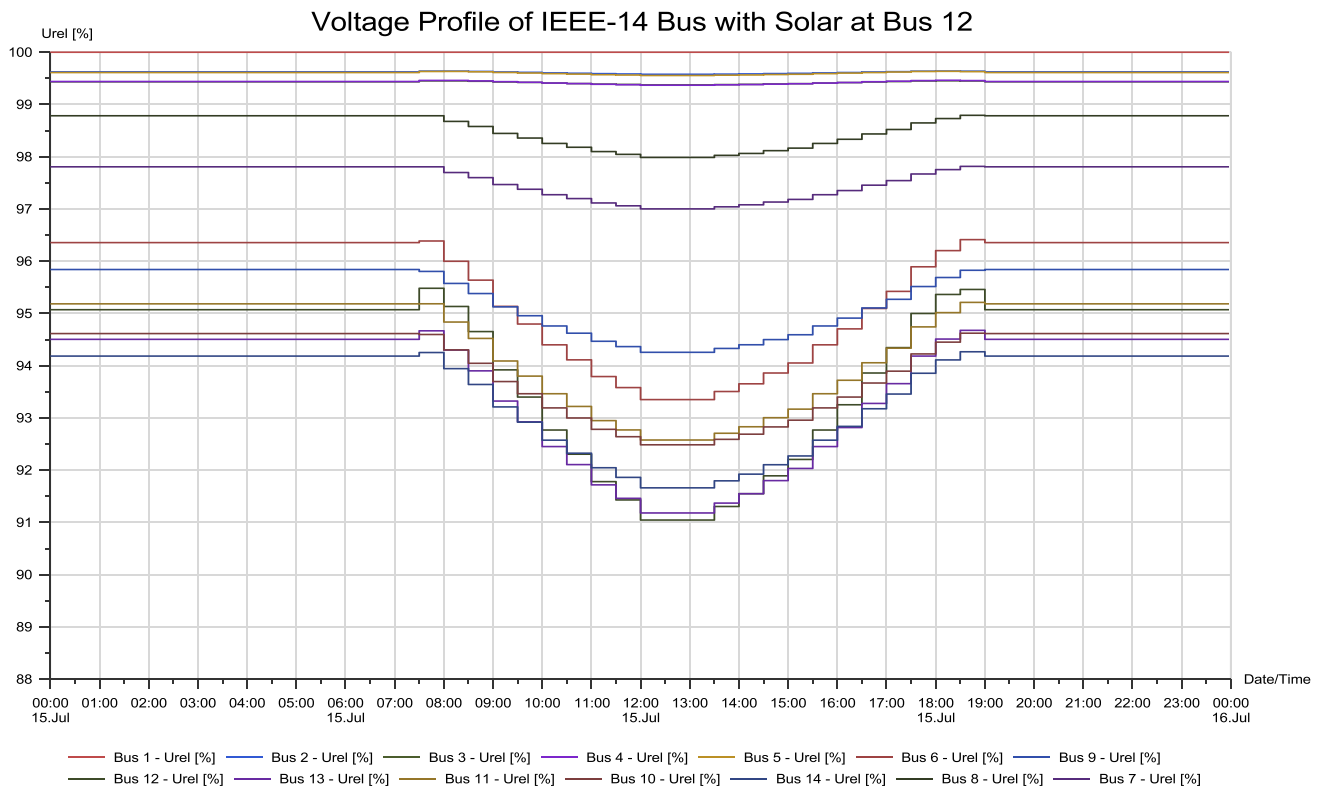


Fig. 6 Voltage profile of IEEE-14 bus with solar at bus 12

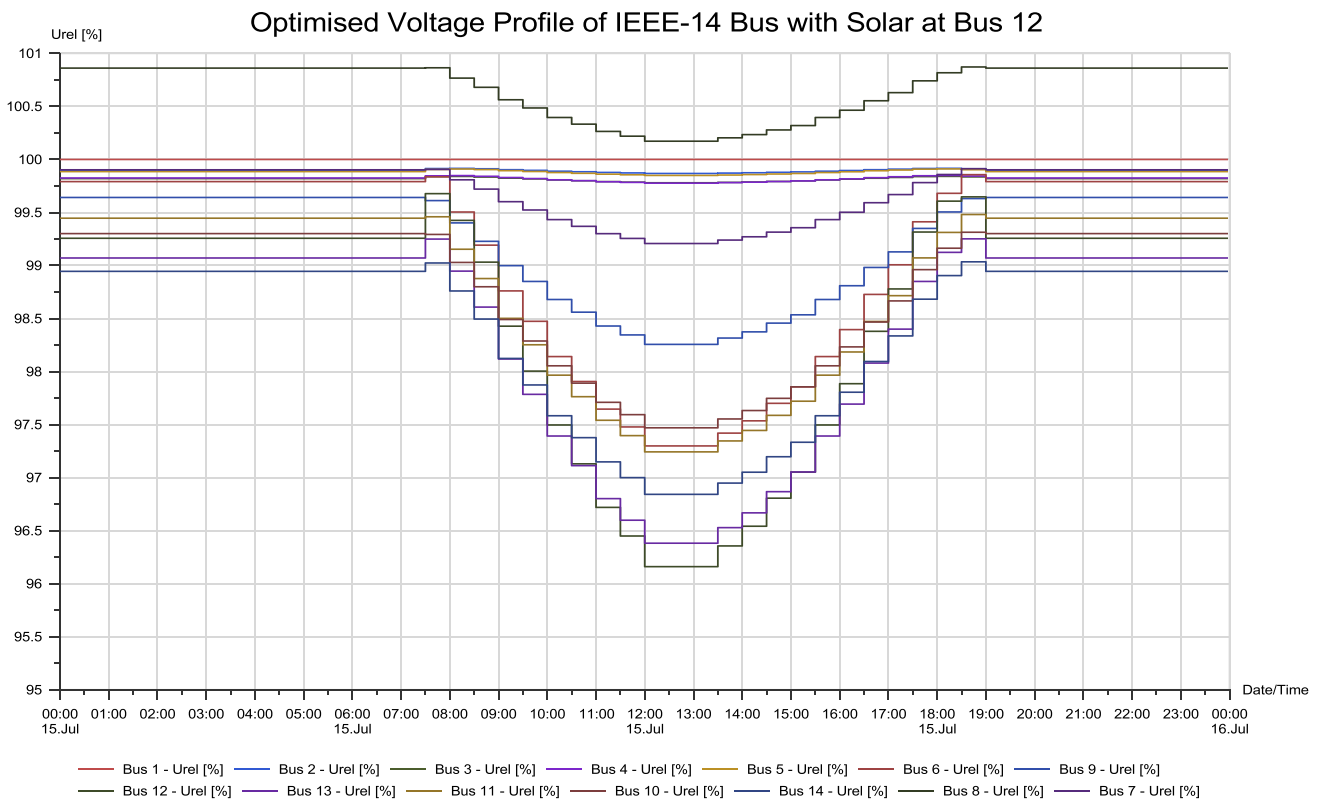


Fig. 7 Voltage profile of IEEE-14 bus after optimal allocation of capacitors

Table 6 Results of optimised placement of capacitors for reactive power demand

Bus	Qn [MVar]
2	- 6.71
3	- 13.15
5	- 1.6
6	- 5.02
9	- 16.72
12	- 1.62
13	- 5.91
11	- 1.82
10	- 5.88
14	- 5.11

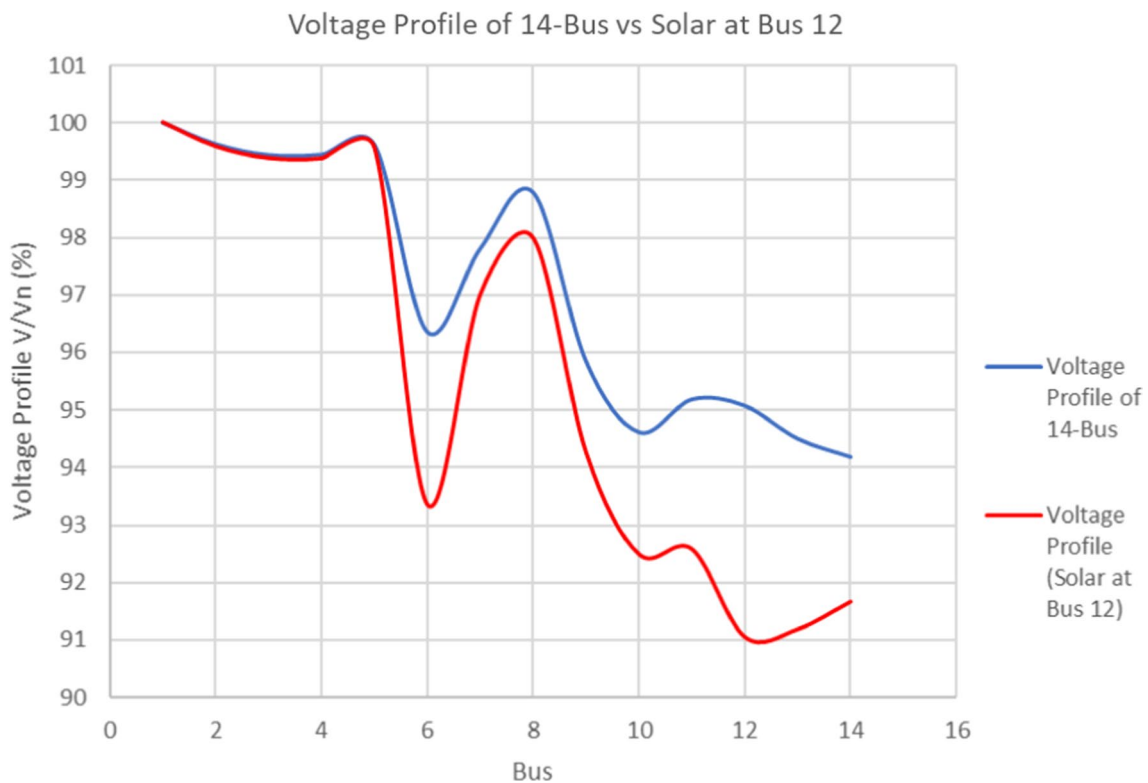
data of voltage at each bus when there is no solar power compared to that of with solar power. Figure 9 demonstrates the improvement of these bus voltage data after capacitors were placed optimally in the buses of the IEEE-14 bus based on the specific locations and reactive power demand ratings of the optimal configuration.

4.3 Management of reactive power flow by optimal allocation of capacitors

When load flow analysis was carried out on the IEEE-14 bus, the power flow in terms of real power (P), reactive power (Q), and apparent power (S) were evaluated based on the buses. Real power with a positive value is equivalent to feeding while real power with a negative value is equivalent to removing real power. Power flow to the bus is positive and the power flow away from the bus is negative. Positive reactive power is equivalent to capacitive feeding while negative reactive power is equivalent to inductive removal of reactive power. The results of power flow for the system without solar power penetration are tabulated in Table 8.

Table 7 Voltage profile changes in the IEEE 14-bus system

Bus	V/V _n (%) of IEEE-14 bus without solar penetration at all periods in a day	V/V _n (%) of IEEE-14 bus at 12 p.m. with solar power penetration at bus 12	V/V _n (%) of the IEEE-14 bus at 12 p.m. after compensation optimisation
1	100	100	100
2	99.624	99.578	99.868
3	99.434	99.376	99.78
4	99.44	99.37	99.777
5	99.611	99.555	99.849
6	96.355	93.351	97.299
7	97.807	97.001	99.207
8	98.784	97.986	100.172
9	95.841	94.256	98.256
10	94.615	92.486	97.47
11	95.183	92.576	97.243
12	95.072	91.045	96.161
13	94.503	91.181	96.382
14	94.184	91.661	96.842

**Fig. 8** Voltage profile of 14-Bus vs 14-Bus with solar at bus 12

With the penetration of intermittent solar power in bus 12, a variation of power flow results was obtained based on time. In this case, the peak period of sunshine and voltage profile which is 12 p.m. was used as the benchmark to compare the worse cases of power flow. Table 9 shows the power flow when the solar bus was integrated into bus 12 at 12 p.m.

From these power flow results; the real and reactive power remained constant throughout for all the buses except for bus 1. In terms of real power, bus 1 had a real power of 107.087 MW and it dropped to 46.406 MW after the penetration of solar power. There was a rise in reactive power in bus 1 from 64.419 MVAR to 91.61 MVAR at 12 p.m. due

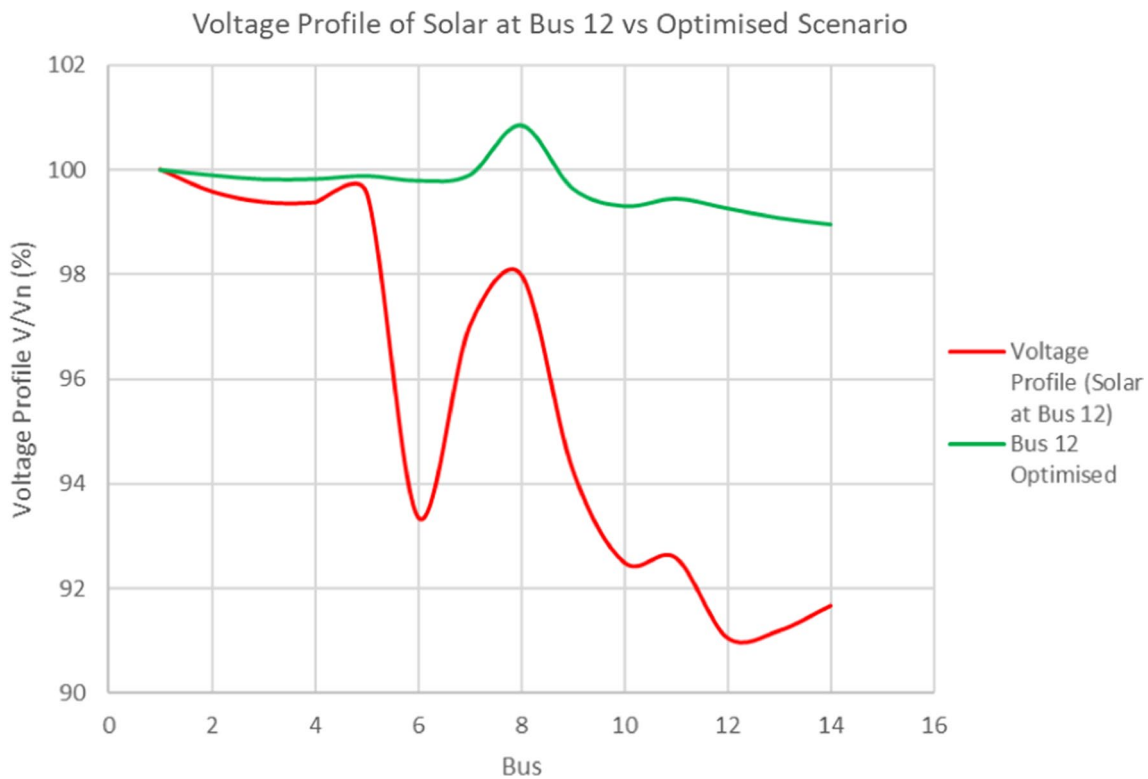


Fig. 9 Voltage profile of 14-bus with solar at bus 12 vs optimised scenario of capacitor placements

Table 8 Power flow results of IEEE-14 bus without solar

Bus	P [MW]	Q [MVar]	S [MVA]
1	107.087	64.419	124.97
2	32.3	- 6.7	32.988
3	- 40.2	- 13.1	42.281
4	- 47.8	3.9	47.959
5	- 7.6	- 1.6	7.767
6	11.3	- 5	12.357
7	0	0	0
8	22.5	2.5	22.638
9	- 29.5	- 16.6	33.85
10	- 9	- 5.8	10.707
11	- 3.5	- 1.8	3.936
12	- 6.1	- 1.6	6.306
13	- 13.8	- 5.8	14.969
14	- 14.9	- 5	15.717

to solar power penetration. After the capacitors were placed, the results for power flow were obtained for comparison purposes as the pattern of fluctuation in power was uniform throughout all buses as shown in Table 10. It was observed that the reactive power in bus 1 was reduced from 91.61 MVar to 22.167 MVar at 12 p.m. after the capacitors were placed. There was a slight reduction in real power of 46.406 MW to 45.967 MW in bus 1 at this period.

Figure 10 illustrates the change in the reactive power flow in all 14 buses at the peak period of 12 p.m. with solar penetration compared to the optimised scenario. Figures 11, 12, and 13 illustrate the time series results of real and reactive power in Bus 1 based on the three cases.

Table 9 Power flow results of IEEE-14 bus with the solar bus at bus 12 at 12 p.m

Bus	P [MW]	Q [MVar]	S [MVA]
1	46.406	91.61	102.694
2	32.3	- 6.7	32.988
3	- 40.2	- 13.1	42.281
4	- 47.8	3.9	47.959
5	- 7.6	- 1.6	7.767
6	11.3	- 5	12.357
7	0	0	0
8	22.5	2.5	22.638
9	- 29.5	- 16.6	33.85
10	- 9	- 5.8	10.707
11	- 3.5	- 1.8	3.936
12	- 6.1	- 1.6	6.306
13	- 13.8	- 5.8	14.969
14	- 14.9	- 5	15.717

Table 10 Power flow results of IEEE-14 bus after capacitor placement at 12 p.m

Bus	P [MW]	Q [MVar]	S [MVA]
1	45.967	22.167	51.033
2	32.3	- 0.004	32.3
3	- 40.2	- 0.01	40.2
4	- 47.8	3.9	47.959
5	- 7.6	- 0.001	7.6
6	11.3	- 0.247	11.303
7	0	0	0
8	22.5	2.5	22.638
9	- 29.5	- 0.458	29.504
10	- 9	- 0.212	9.002
11	- 3.5	- 0.079	3.501
12	- 6.1	- 0.098	6.101
13	- 13.8	- 0.311	13.803
14	- 14.9	- 0.21	14.901

4.4 Improvement of voltage profile in the IEEE-14 bus by volt-var regulation

After implementing this function in the solar bus, the buses resulted in a steadier voltage, and its levels were also improved but some buses were still below 0.95 p.u. In the results, instead of only increasing the levels of the voltage profile with the capacitors which had an estimated average voltage deviation of 2.828% for all buses, the implementation of the volt-var function in the solar bus resulted in approximately the same levels of voltage profile but with a smaller deviation of approximately 1.3% as average for all buses. Figures 14 and 15 demonstrate these results in which the voltage deviation from its initial point (12 a.m.) is reduced after the implementation of the volt-var function. Figure 16 and Table 11 show the voltage profile results of all the scenarios.

Comparatively, the average voltage profile of all the buses (at 12 p.m.) of the IEEE-14 bus (without solar power) had an average value of 97.18% and this was reduced to 95.67% after solar was connected to bus 12 in which there were buses that violated the grid code requirements of below 0.95 p.u. This can be observed in the illustration of the time-series graph in Fig. 6. Table 11 shows the voltage profile of each bus taken at a reference period of 12 p.m. This value was improved to 98.45% after the optimal placement of capacitors but the voltage was not a steady (constant line) as seen in Fig. 7. With volt-var regulation, the average voltage profiles of all buses showed improvement from 95.67% to 96.89% and a steadier voltage can be observed based on Fig. 15. For the case of using both optimal

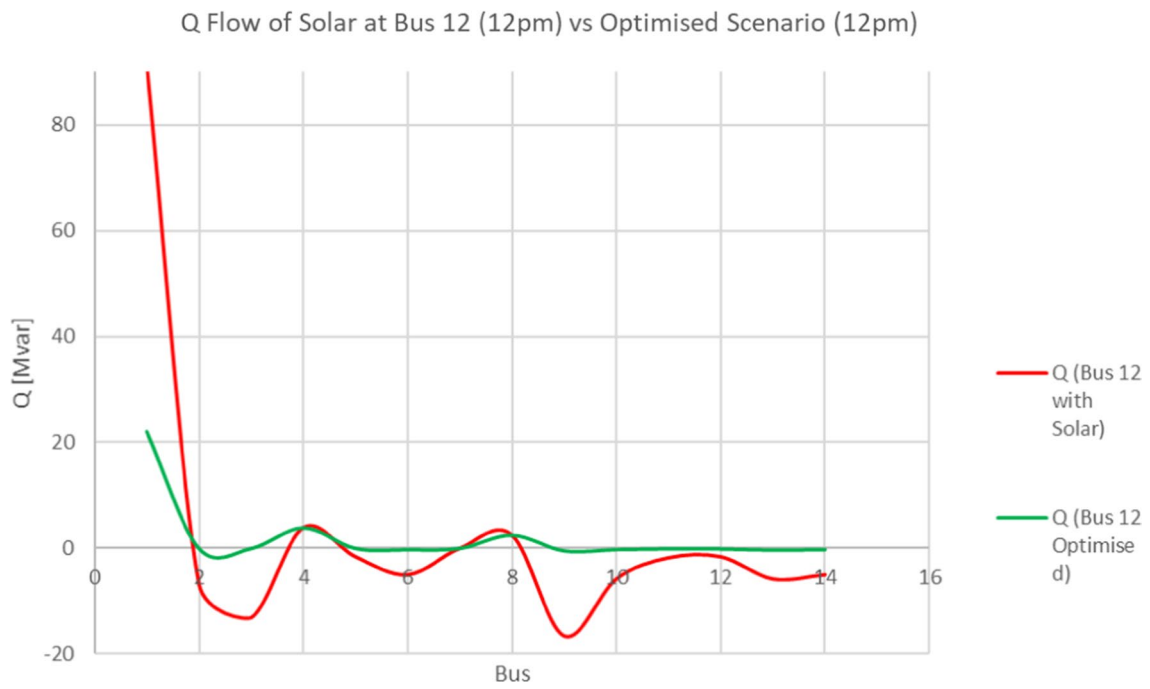


Fig. 10 Minimisation of reactive power flow in all buses when 14-bus with solar at bus 12 is compensated with the optimal allocation of capacitors at 12 p.m

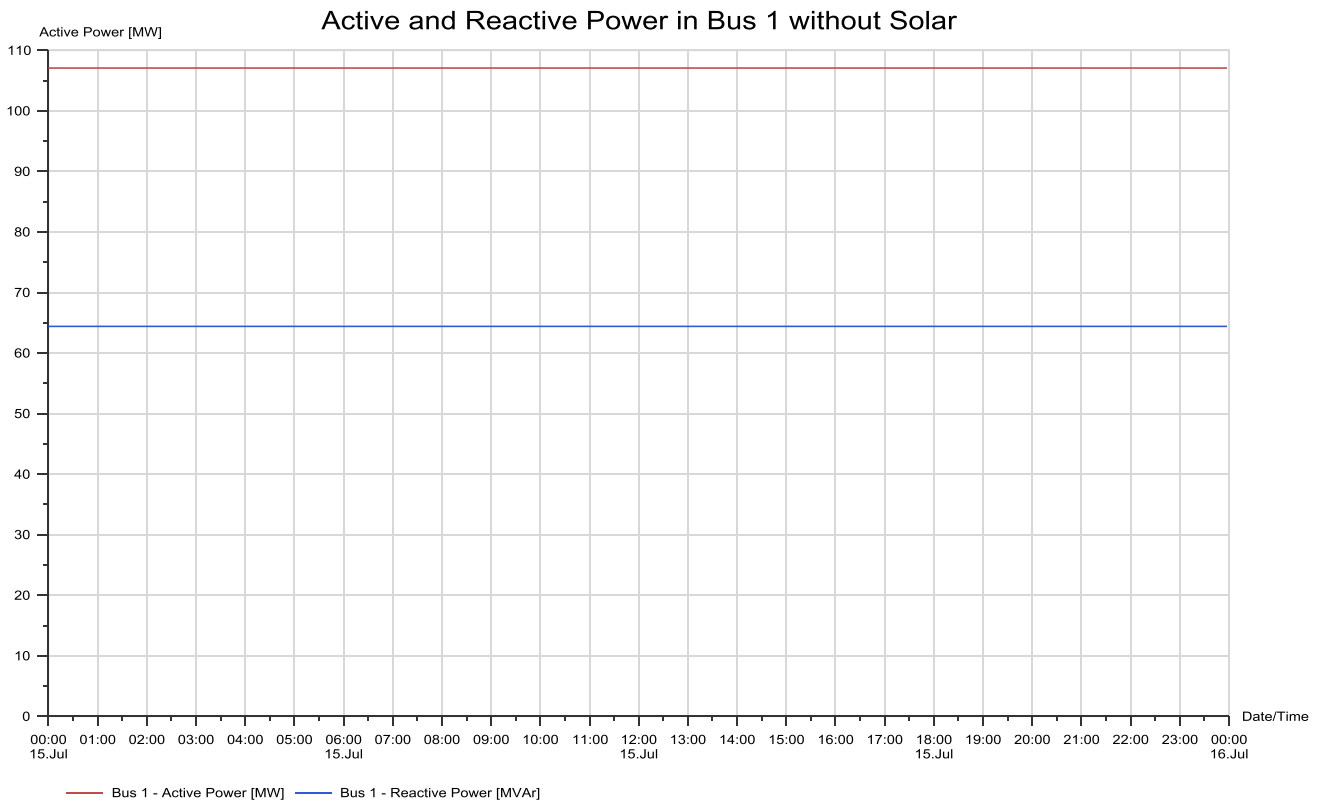


Fig. 11 Time series active and reactive power flow in bus 1 without solar power penetration

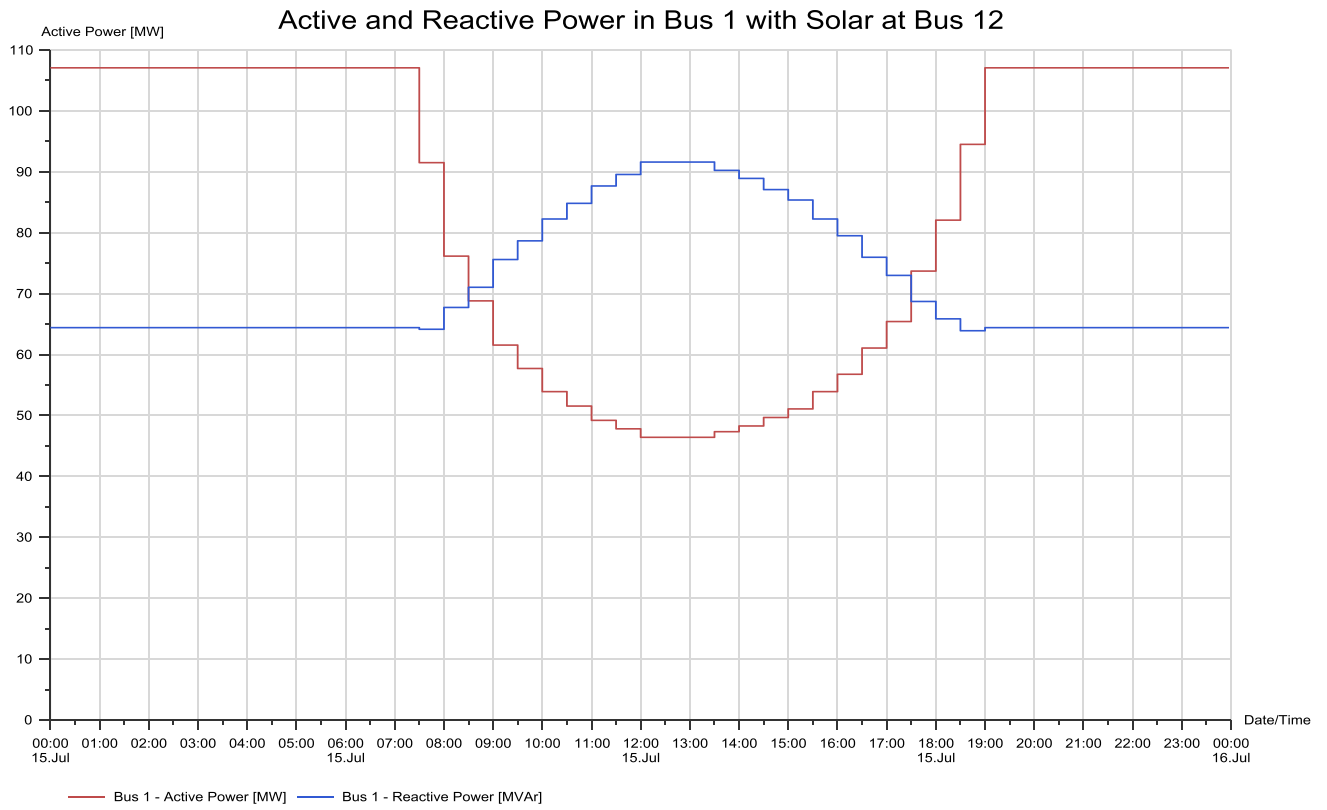


Fig. 12 Time series active and reactive power flow in bus 1 with solar bus at bus 12

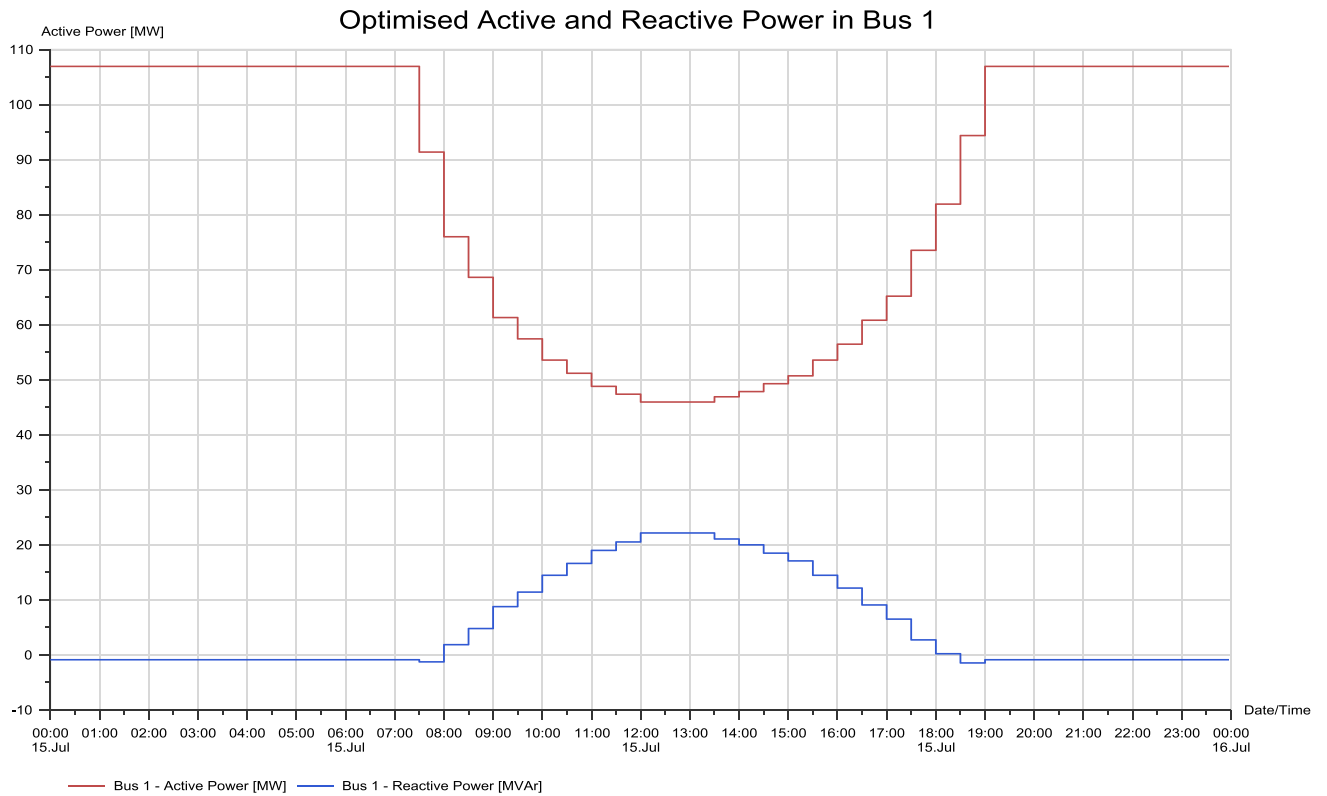


Fig. 13 Time series active and reactive power flow in bus 1 after optimal allocation of capacitors

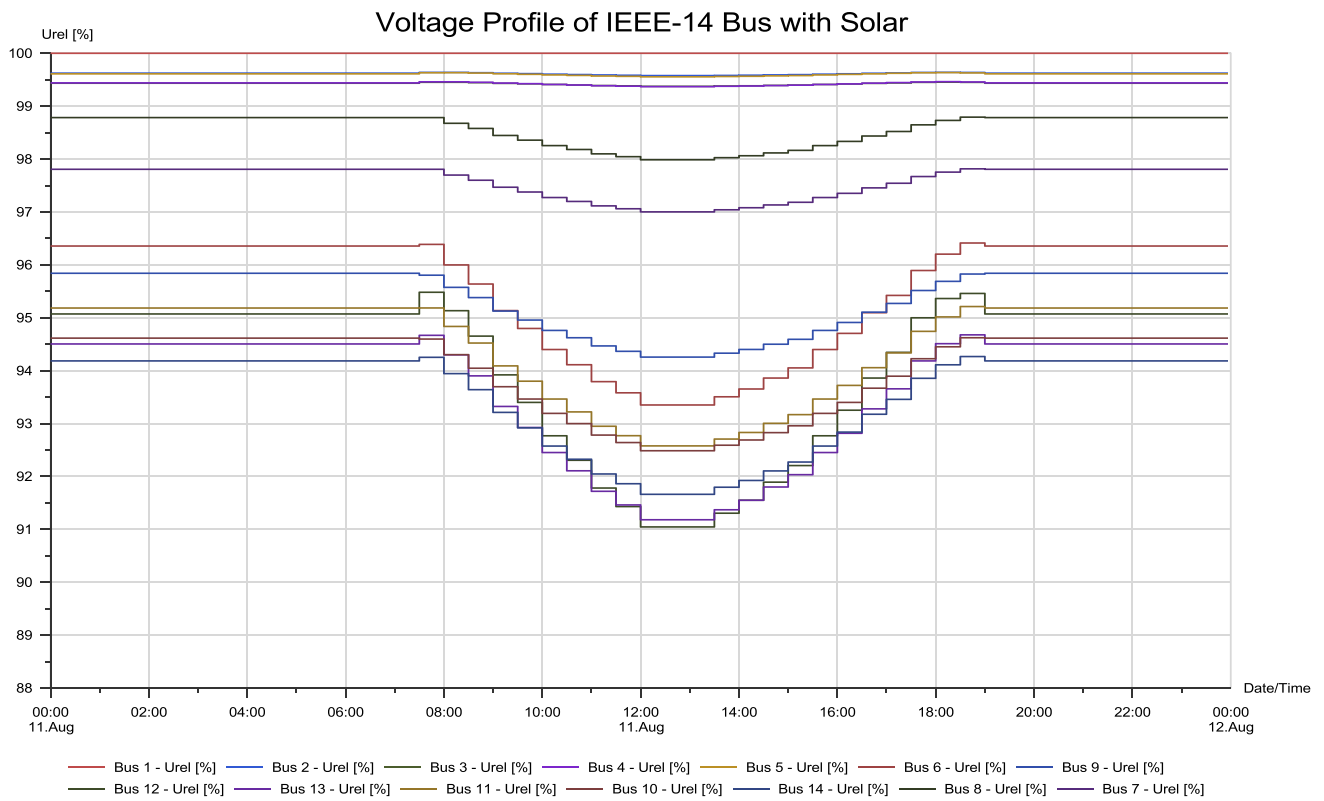


Fig. 14 Voltage profile of IEEE-14 bus with solar integration (without volt-var function)

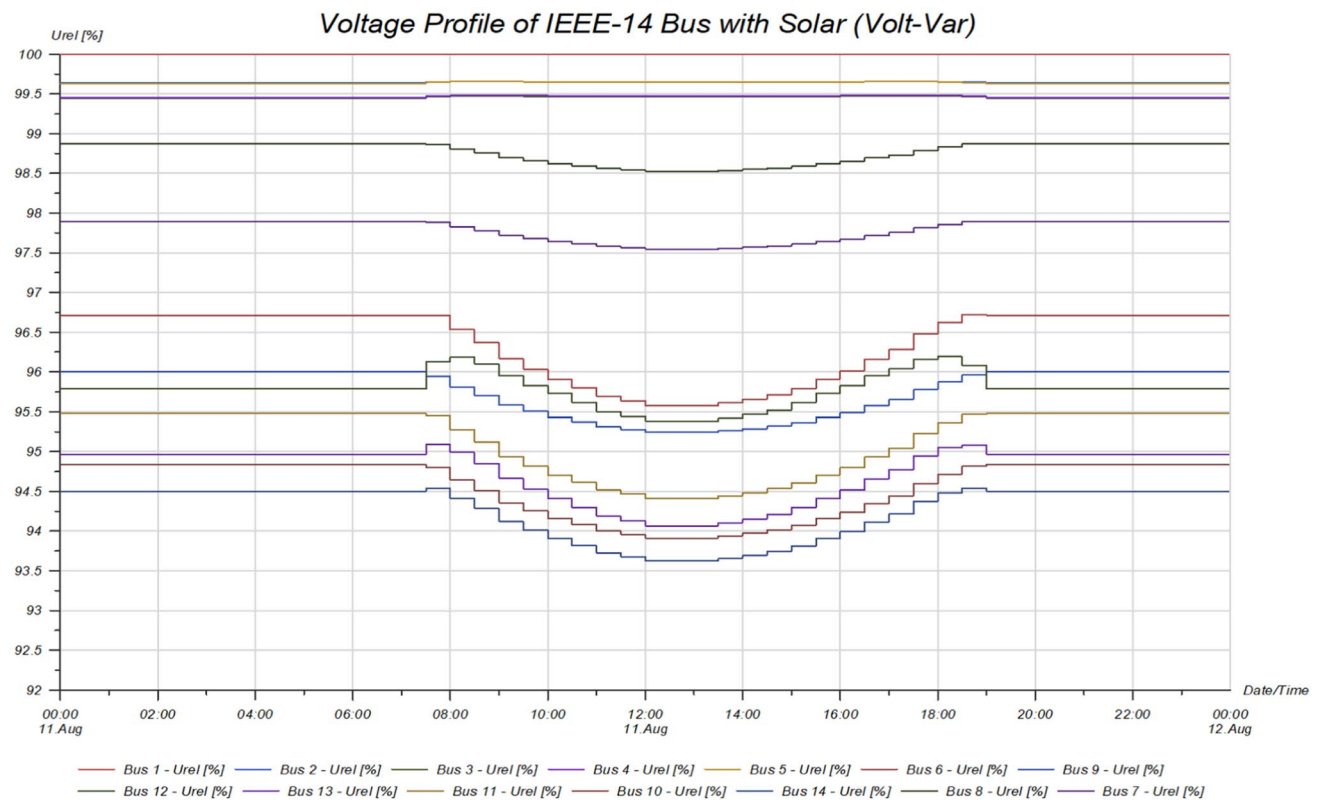


Fig. 15 Voltage profile of IEEE-14 bus with volt-var regulation on the solar bus

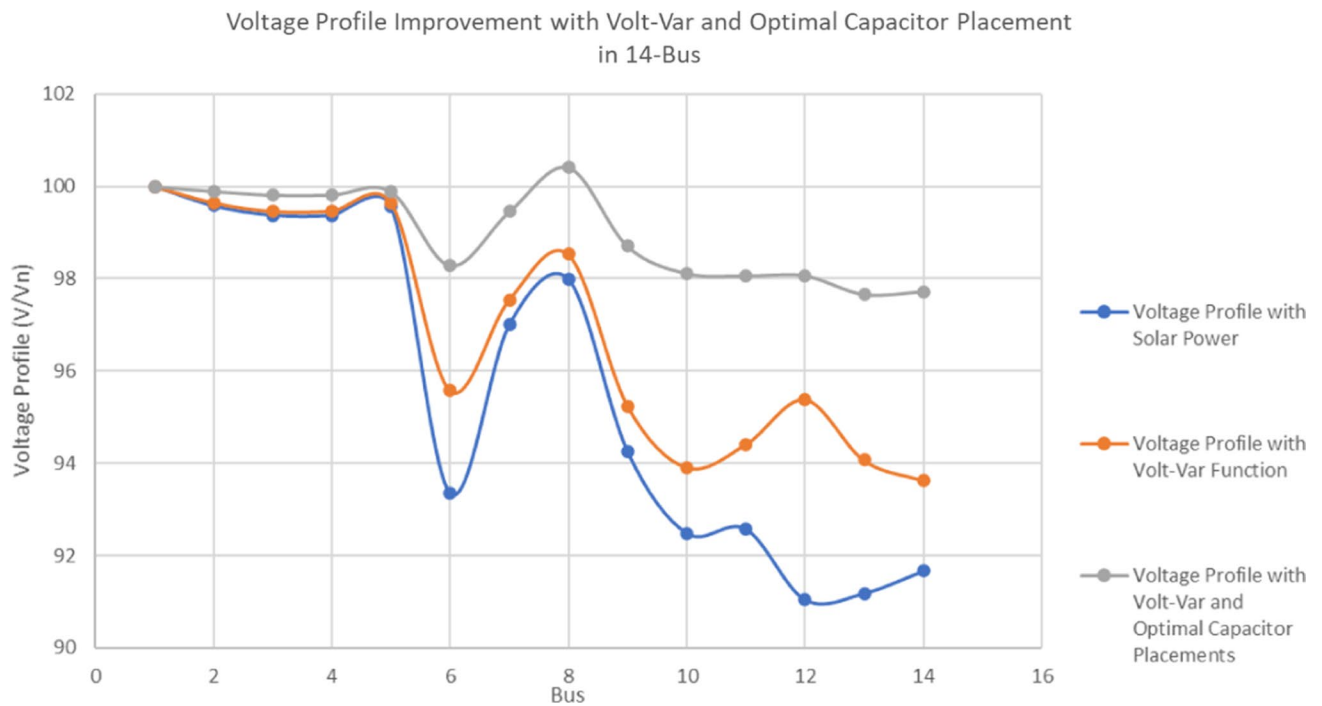


Fig. 16 Voltage profile improvement with volt-var and optimal capacitor placements

Table 11 All scenarios of voltage profile in the IEEE-14 bus topology

Bus	V/Vn (%) of 14-bus without solar power	V/Vn (%) of 14-bus with solar power	V/Vn (%) of 14-bus after optimal allocation of capacitors	V/Vn (%) of 14-bus after volt-var regulation	V/Vn (%) of 14-bus after volt-var regulation and optimal allocation of capacitors
1	100.000	100	100	100	100
2	99.624	99.578	99.868	99.647	99.899
3	99.434	99.376	99.780	99.461	99.818
4	99.440	99.37	99.777	99.471	99.822
5	99.611	99.555	99.849	99.645	99.889
6	96.355	93.351	97.299	95.576	98.284
7	97.807	97.001	99.207	97.547	99.454
8	98.784	97.986	100.172	98.526	100.417
9	95.841	94.256	98.256	95.243	98.704
10	94.615	92.486	97.470	93.912	98.114
11	95.183	92.576	97.243	94.411	98.063
12	95.072	91.045	96.161	95.384	98.067
13	94.503	91.181	96.382	94.066	97.661
14	94.184	91.661	96.842	93.625	97.722

capacitor allocation and volt-var regulation, the average voltage profile for all buses were improved to be 98.99%. All these results were tabulated in Table 11 which were the overall results obtained for the IEEE-14 bus based on all five cases of solar power penetration and reactive power management.

5 Conclusion

This research aimed to investigate the issues of voltage profile in the IEEE-14 bus when time-varying solar power was injected into this test bed system. The issues of solar power intermittency were discussed to understand the complexity and various causes of this random nature of VRE sources. A review of the literature regarding power system stability of electrical networks with penetration of solar power was carried out followed by the recent work on the optimal allocation of reactive power compensation devices and solar inverters. For the methods used in this research, power flow analysis, optimal allocation of capacitors, and volt-var regulation were carried out to study the power flow, reactive power demands, voltage profile drop by injection of variable solar power, reactive power ratings, and injections of reactive power by capacitor banks that were optimally placed in the network, and improvement in steadiness of voltages throughout the day. From the results obtained, it was found that the connection to bus 12 demonstrated the lowest voltage profile cases. The average value of the voltage profile for all buses of the IEEE 14-bus system demonstrated a reduction of 3.29% as taken from 7 a.m. to 12 p.m. (maximum to minimum voltage profile throughout the day). With the optimum allocation of the capacitors, the voltage levels in all weak buses of the IEEE-14 bus were increased to be between 0.95 p.u. to 1.05 p.u. which was the voltage specifications of the Malaysian Grid Code Requirements. The voltage for every weak bus in the IEEE-14 bus showed a rise of 5.7% from 7 a.m. to 12 p.m. With that, the volt-var function was used for reactive power regulation at the point of common coupling (PCC) and a reduction of voltage deviation of 2.828% to 1.3% in the IEEE-14 bus was observed. The average voltage profile of all buses managed to attain a value of 98.99% from 95.673% (with solar power) by using both methods of the optimal allocation of capacitors and volt-var regulation.

5.1 Recommendations and future works

Research in [24, 25] carried out a comprehensive review of literature on the optimal location and sizing of reactive power compensation devices. Furthermore, issues in grid integration with solar PV and utility storage sizing were reviewed in [26–29]. There are future works and recommendations based on the literature and methods covered in this scope of research as follows:

- Planning of reactive power compensation devices in electrical networks with numerous VRE generators connected at different buses can be solved by various heuristic algorithms to get optimum of reactive power flow, voltage, and power quality delivered to loads.
- Efficiency of real-time control algorithms utilised in the characteristics of convergence rate, computation time, and number of iterations. More investigation on issues of reactive power management with VRE generators by novel metaheuristic approaches, conventional approaches, analytical approaches, and hybrid-based approaches [24].
- The coordinated control and coordination of smart inverters to provide reactive power support can enhance grid stability. The integration adaptive algorithms into these inverters allows them to adapt their reactive power control based on the system dynamics and grid conditions which evolve as different levels of VRE are injected into the grid at different periods of time.

Author contributions MIZ involved in data analysis, interpretation of data and manuscript writing, GYI involved in supervision, design of the work, manuscript revision.

Data availability The datasets generated during and/or analysed during the current study are available from the corresponding author on reasonable request.

Declarations

Competing interests The authors declare no competing interests.

Open Access This article is licensed under a Creative Commons Attribution 4.0 International License, which permits use, sharing, adaptation, distribution and reproduction in any medium or format, as long as you give appropriate credit to the original author(s) and the source, provide a link to the Creative Commons licence, and indicate if changes were made. The images or other third party material in

this article are included in the article's Creative Commons licence, unless indicated otherwise in a credit line to the material. If material is not included in the article's Creative Commons licence and your intended use is not permitted by statutory regulation or exceeds the permitted use, you will need to obtain permission directly from the copyright holder. To view a copy of this licence, visit <http://creativecommons.org/licenses/by/4.0/>.

References

1. SEDA. Malaysia renewable energy roadmap, pathway towards low carbon energy system, 2021; https://www.seda.gov.my/reportal/wp-content/uploads/2021/12/MyRER_webVer-1.pdf. Accessed 5 May 2023.
2. Chalmers SM, Hitt MM, Underhill JT, Anderson PM, PL Vogt PL, R Ingersoll R. IEEE Transactions on Power Apparatus and Systems, 1985; p.524.
3. Li W, Ren H, Chen P, Wang Y, Qi H. Key operational issues on the integration of large-scale solar power generation—a literature review. *Energies*. 2020. <https://doi.org/10.3390/en13225951>.
4. Shah R, Mithulananthan N, Bansal RC, Lee KY, Lomi A, Power system voltage stability as affected by large-scale PV generation, Proceedings of the 2011 International Conference on Electrical Engineering and Informatics, IEEE, 2011; p. 1 <https://doi.org/10.1109/ICEEI.2011.6021723>.
5. IRENA. Scaling Up Variable Renewable Power: The Role of Grid Codes, Abu Dhabi. 2016.
6. Shah R, Mithulananthan N, Bansal RC. Oscillatory stability analysis with high penetrations of large-scale photovoltaic generation. *Energy Conv and Manag*. 2012;65:420. <https://doi.org/10.1016/j.enconman.2012.08.004>.
7. Khan R, Go YI. Assessment of Malaysia's large-scale solar projects: power system analysis for solar PV grid integration. *Global Chall*. 2020. <https://doi.org/10.1002/gch2.201900060>.
8. Shah R, Nadarajah M, Bansal R, Lee KY, Lomi A. Influence of large-scale PV on voltage stability of sub-transmission system. *Int J Electrical Eng Inf*. 2012;4(1):148–61. <https://doi.org/10.15676/ijeel.2012.4.1.12>.
9. Kabir S, Krause O, Bansal R, Ravishanker J. Dynamic voltage stability analysis of sub-transmission networks with large-scale photovoltaic systems; IEEE, 2014; pp. 1–5. <https://doi.org/10.1109/PESGM.2014.6938877>.
10. Muhammad Y, Arbab MN, Optimization in tap changer operation of power transformer using reactive power compensation by FACT devices, IEEE 4th Control and System Graduate Research Colloquium, 2013; pp. 27–31. <https://doi.org/10.1109/ICSGRC.2013.6653270>.
11. Huchche VA, Salodkar PA, Manumare P, Reactive power compensation of grid-connected PV system', Shri Ramdeobaba College of Engineering and Management, 2019; pp. 1–6. <https://doi.org/10.29042/2019-5836-5840>.
12. Zakutsky VI, Gadzhiev MG, Yermolov NS, Analysis of the influence of installed FACTS devices and transformer on-load tap changers (OLTC) in transmission networks on a total power losses Unified Energy System (UES) of Russia', 2019 *International Youth Conference on Radio Electronics, Electrical and Power Engineering (REEPE)*, 2019; pp. 1–6 <https://doi.org/10.1109/REEPE.2019.8708847>.
13. Mohanan M, Go YI. Optimised power system management scheme for LSS PV grid integration in Malaysia using reactive power compensation technique. *Glob Chall*. 2020;4(4):1–12. <https://doi.org/10.1002/gch2.201900093>.
14. Peprah F, Gyamf S, Efah-Donyina E, Amo-Boateng M. Evaluation of reactive power support in solar PV prosumer grid. *Prime Adv Electr Eng Electron Energy*. 2022;2:100057. <https://doi.org/10.1016/j.prime.2022.100057>.
15. Pereira LDL, Yahyaoui I, Fiorotti R, de Menezes LS, Fardin JF, Rocha HRO, Tadeo F. Optimal allocation of distributed generation and capacitor banks using probabilistic generation models with correlations. *Appl Energy*. 2022;307: 118097. <https://doi.org/10.1016/j.apenergy.2021.118097>.
16. Souri S, Shourkaei HM, Soleymani S, Mozafari B. Flexible reactive power management using PV inverter overrating capabilities and fixed capacitor. *Electr Power Syst Res*. 2022;209: 107927. <https://doi.org/10.1016/j.epsr.2022>.
17. Nusair K, Alasali F, Hayajneh A, Holderbaum W. Optimal placement of FACTS devices and power-fow solutions for a power network system integrated with stochastic renewable energy resources using new metaheuristic optimization techniques. *Int J Energy Res*. 2021;45(13):18786–809. <https://doi.org/10.1002/er.6997>.
18. Jurák V, Bukvišová Z, Orságová J, Topolánek D, Ptáček M. Compensation of reactive power in LV network and its impact on reactive power fow through distribution grid. In: 2020 21st international scientific conference on electric power engineering (EPE). Prague: Prague, Czech Republic CVUT—Czech Technical University in Prague; 2020. p. 1–5.
19. Fernandez MI, Go YI, Power management scheme development for large-scale solar grid integration. *Journal of Electrical Systems and Information Technology*, 2023; 10, [15] <https://doi.org/10.1186/s43067-023-00080-7>.
20. Grid code for Peninsular Malaysia, Suruhanjaya Tenaga, Malaysia, 2016; pp. 168–186.
21. Siemens, 'PSS SINICAL 17.0 Power flow: power flow calculations in electrical networks', Siemens AG, 2021; p. 39.
22. Siemens 'PSS SINICAL 17.0 Optimisations: determination of optimisations in electrical networks', Siemens AG, 2021; pp. 21–28.
23. IEEE-14 Bus Data Sheet 'Datasheet for IEEE-14 bus system', App. A, 2017; pp. 126–128.
24. Ismail F, Abdul Wahab NI, Othman ML, Radzi MAM, Naidu Vijayakumar K, Mat Naain K. (2020) 'A Comprehensive Review on Optimal Location and Sizing of Reactive Power Compensation Using Hybrid-Based Approaches for Power Loss Reduction, Voltage Stability Improvement, Voltage Profile Enhancement and Loadability Enhancement', in IEEE Access, vol. 8, pp. 222733-222765, doi: <https://doi.org/10.1109/ACCESS.2020.3043297>.
25. Yeoh CK, Go YI (2023) Investigation of voltage profile variation and stability of PV-grid interconnected system. In: Choo CS, Wong BT, Sharkawi KHB, Kong D (eds) Proceedings of ASEAN-Australian Engineering Congress (AAEC2022). AAEC 2022. Lecture Notes in Electrical Engineering, vol 1072. Springer, Singapore. https://doi.org/10.1007/978-981-99-5547-3_19.
26. Shafiullah M, Ahmed SD, Al-Sulaiman FA. Grid integration challenges and solution strategies for solar PV systems: a review. *IEEE Access*. 2022;10:52233–57. <https://doi.org/10.1109/ACCESS.2022.3174555>.

27. Thadani HL, Go YI (2021) Integration of solar energy into low-cost housing for sustainable development: case study in developing countries, vol 7, no 12. *Heliyon*, Elsevier, p e08513. <https://doi.org/10.1016/j.heliyon.2021.e08513>.
28. Thadani HL, Go YI (2023) Large-scale solar system design, optimal sizing and techno-economic environmental assessment. *Sustain Energy Res* 10:11. <https://doi.org/10.1186/s40807-023-00081-0>.
29. Choo BL, Go YI (2022) Energy storage for large scale/utility renewable energy system - an enhanced safety model and risk assessment. *Renew Energy Focus* 42:79–96. <https://doi.org/10.1016/j.ref.2022.05.001>.

Publisher's Note Springer Nature remains neutral with regard to jurisdictional claims in published maps and institutional affiliations.